

Effect of suppressed excitation on the amplitude distribution of 5-min oscillations in sunspots

Parchevsky, K.V., Kosovichev, A.G.

W.W. Hansen Experimental Physics Laboratory, Stanford University, Stanford, CA, USA

ABSTRACT

Five-minute oscillations on the Sun (acoustic and surface gravity waves) are excited by subsurface turbulent convection. However, in sunspots the excitation is suppressed because strong magnetic field inhibits convection. We use 3D simulations to investigate how the suppression of excitation sources affects the distribution of the oscillation power in sunspot regions. The amplitude of random acoustic sources was reduced in circular-shaped regions to simulate the suppression in sunspots. The simulation results show that the amplitude of the oscillations can be approximately 2-4 times lower in the sunspot regions in comparison to the quiet Sun, just because of the suppressed sources. Using SOHO/MDI data we measured the amplitude ratio for the same frequency bands outside and inside sunspots, and found that this ratio is approximately 3-4. Hence, the absence of excitation sources inside sunspots makes a significant contribution (about 50% or higher) to the observed amplitude ratio and must be taken into account in sunspot seismology.

Subject headings: Sun: oscillations—sunspots

1. Introduction

It has been known for a long time that 5-min solar oscillations have significantly lower amplitude (by a factor of 2-5) in sunspots and plages than in the quiet Sun (e.g. Woods & Cram 1981; Thomas et al. 1982; Title et al. 1992). Hindman (1997) enumerated four possible mechanisms to explain the observed power suppression: 1) reduction of excitation of p-modes inside sunspots; 2) absorption of p-modes inside sunspots (e.g. Cally 1995); 3) the different height of spectral line formation due to the Wilson depression; 4) altering of p-mode eigenfunctions by the magnetic field. The precise contribution of these effects to the observed amplitude reduction is still unknown. In this paper we study the first effect: changes in the oscillation amplitude due to suppression of acoustic sources by using

3D numerical simulation of solar acoustic waves, which are important for solar seismology studies. Inside sunspots, strong magnetic field inhibits turbulent convective motions which are the source of the 5-min solar oscillations. Therefore, the waves in the 5-min period (3 mHz frequency) range, observed in sunspots, mostly come from the outside regions, and thus their amplitude is reduced in comparison to the quiet Sun. Our goal was to estimate the significance of this effect by modeling wave fields in horizontally uniform background solar models with regions of reduced excitation. The main result is that the suppression of oscillation sources inside sunspots can make substantial (about 50% or greater) contribution to the reduction of amplitude inside sunspots, and thus must be taken into account in sunspot seismology.

2. Method

Wave propagation on the Sun (in absence of magnetic field and flows) can be described by the following system of linearized Euler equations:

$$\begin{aligned} \frac{\partial \rho'}{\partial t} + \nabla \cdot (\rho_0 \mathbf{u}') &= 0 \\ \frac{\partial}{\partial t}(\rho_0 \mathbf{u}') + \nabla p' &= \mathbf{g}_0 \rho' + \mathbf{f}(x, y, z, t), \end{aligned} \tag{1}$$

where u', v', w' are the perturbations of x, y, z velocity components, ρ' and p' are the density and pressure perturbations correspondingly, $\mathbf{f}(x, y, z, t)$ is the function describing the acoustic sources. The pressure p_0 , density ρ_0 , and gravitational accelerations \mathbf{g}_0 of the background reference model depend only on depth z . We used the adiabatic relation $\delta\rho/\rho_0 = 1/\Gamma_1 \delta p/p_0$ between Lagrangian variations of pressure δp and density $\delta\rho$. The adiabatic exponent Γ_1 was calculated from OPAL equation of state (Rogers et al. 1996).

The numerical method is based on a high-order finite difference scheme, developed by Tam & Webb (1993) and described in details by Parchevsky & Kosovichev (2006). The coefficients of this finite difference scheme are chosen to minimize the error of the Fourier transform of numerical derivatives. Such a scheme preserves the dispersion relations of the continuous case for shorter wavelengths. A 3rd-order strong stability preserving Runge-Kutta method (Shu 2002) was used for time integration.

The standard solar model (Christensen-Dalsgaard et al. 1996) with a smoothly joined chromospheric model of Vernazza et al. (1976) was used as the background state. The model was corrected in the near-surface layers to prevent development of convective instability in the superadiabatic layer by replacing large negative values of the Brunt-Väisälä frequency by zero (or small positive) values and recalculating the hydrostatic equilibrium

(Parchevsky & Kosovichev 2006). This is a necessary modification for all linear simulations of this type. It suppresses rapidly growing unstable convective modes but does not affect essential properties of acoustic wave propagation in the Sun.

To prevent reflection of acoustic waves from the boundaries of the computational domain, we follow the PML (Perfectly Matching Layer) method of Hu (1996). We set the top non-reflecting boundary condition above the temperature minimum. This simulates a realistic case when the waves are only partially reflected by the photosphere. The waves with frequencies higher than acoustic cut-off frequency $\nu_{ac} \sim 5$ mHz pass through the photosphere and are absorbed by the PML. For frequencies below ν_{ac} , the top boundary does not affect the reflection because the acoustic waves are mostly reflected by the photosphere and become evanescent in the chromosphere.

The damping mechanism of solar modes below the acoustic cut-off frequency is not yet completely understood. It can be due to wave scattering on turbulence in subsurface layers (e.g. Murawski 2003) and also due to partial escape of waves and radiative losses (Christensen-Dalsgaard & Frandsen 1983). We have investigated both of these mechanisms. The atmospheric damping was modeled by imposing the upper absorbing boundary at different levels, and choosing the height of this boundary in such a way (about 500 km above the photosphere) that the observed line widths in the oscillation power spectrum are well reproduced. To model the subsurface (turbulent) damping we followed Gizon & Birch (2002) and added a friction-type term $-\sigma(z)\rho_0v_z$ to the vertical component of momentum equation, where damping coefficient $\sigma(z)$ is constant above the photosphere and smoothly decreases to zero at a depth of about 500 km. For this case, the upper boundary was placed at the chromosphere-corona transition layer (about 1750 km above the photosphere), and the value of $\sigma(z)$ was adjusted to match the observed line widths and relative amplitude of the peaks in the acoustic spectrum. The lateral boundary conditions are periodic. Duration of simulations was 4.5 hours of solar time. We compared results with longer runs and checked that the root mean square (rms) oscillation amplitude reaches an equilibrium state, and also that the simulated acoustic spectra are close to the observed power spectrum.

The question about the depth of the acoustic sources on the Sun is also still open. Numerical simulations of solar convection (Stein & Nordlund 2001) show that in the region around $3 \div 4$ mHz the most driving occurs between the photosphere and sub-surface layer 500 km deep, with a maximum driving at 200-300 km below the surface. Accordingly, the sources were randomly distributed in time and on a horizontal plane 350 km below the photosphere. We considered also the case of shallow (100 km deep) sources, as suggested by Nigam & Kosovichev (1999), Kumar & Basu (2000). The sources were modeled by spherically symmetric Gaussian shape vertical force perturbations with FWHM of 300

km and random amplitudes and frequencies. The time dependence was either a one-period sin function: $\sin[\omega(t - t_0)]$, $t_0 \leq t \leq t_0 + 2\pi/\omega$ or Ricker's wavelet: $(1 - 2x^2)e^{-x^2}$, where $x = [\omega(t - t_0)/2 - \pi]$, $t_0 \leq t \leq t_0 + 4\pi/\omega$. The frequency distribution of acoustic sources was uniform in the range of $2 \div 8$ mHz. The simulations were carried out in the rectangular domain of size $122 \times 122 \times 30$ Mm³ using a uniform $816 \times 816 \times 630$ grid. The simulated and observed power spectra are shown in Fig. 1.

3. Results

Using this method we simulated the distribution of oscillation power for sunspots of various size, acoustic source models, and compared with observations. Observations for sunspots in active regions AR10373 (a,b,c) and AR8243 (d,e,f) obtained by SOHO/MDI are shown in Fig. 2. Panels a) and d) represent maps of the line-of-sight magnetic field from high-resolution MDI data. Panels b) and e) show corresponding vertical velocity oscillation amplitude maps, averaged in the frequency interval $\Delta\nu = 1.2$ mHz with central frequency $\nu = 3.65$ mHz. The azimuthally averaged profiles of the oscillation amplitude (thick solid curves for observations and dashed curves for simulations) and the profile of the source strength (thin solid curves) are shown in panels c) and f).

We simulated the suppression of the acoustic sources (changes in acoustic emissivity) due to magnetic field in sunspots by zeroing the source amplitude at the center of sunspot umbra and smoothly increasing the source strength in the penumbra towards a constant value outside the sunspots (source masking). Numerical experiments with different profiles of the source strength show in all cases that the simulated wave field profile has the shape similar to the profile of the acoustic source strength (this was not a priori obvious). Thus, we use a horizontal profile of the observed wave field (shifted and scaled to be in range $[0,1]$) as an acoustic source strength profile. In reality the strength of acoustic sources depends on magnetic field strength. The actual dependence is unknown, however, the distribution of acoustic sources calculated from the wave field is similar to the inverse profile of the sunspot magnetic field (Fig. 3).

The simulation results (Fig. 2 c,f) show that the waves propagate into the region of reduced excitation, but oscillation amplitude is substantially decreased. However it still does not match the observed values at sunspot center. This means that the suppression of acoustic sources is obviously a very important effect in sunspot seismology. However, other factors are likely to play role too.

The result of simulations for the sunspot in active region AR8243 is shown in Fig. 4.

Panel a) represents the amplitude map for simulations with a low (500 km) top absorbing boundary without explicit damping and filtered with a spatial Gaussian filter with FWHM of 1.5 arcsec to reflect the instrumental smoothing. Panel b) represents the angular averaged amplitude profiles for observations (thick solid curve); simulations with a low top absorbing boundary without explicit damping (thick dashed curve); simulations with a high (1750 km) top absorbing boundary with an additional damping term in the subsurface layers, introduced into the z-component of the momentum equation (thin dashed curve). The thin solid curve shows the strength profile of the acoustic sources. It was shown by Jones (1989) that the height of formation of Ni I 6768 Å line used by the MDI instrument is in the range of 200–300 km above the photosphere. To match the simulations with the MDI observations, the amplitude maps were plotted for the height of 300 km above the photosphere. Velocities V_{in} and V_{out} outside and inside the masked region were calculated by spatial averaging of the amplitude map in the circle of radius 9.0 Mm around the center of the sunspot and outside the sunspot in the ring with inner and outer radii of 45 Mm and 50 Mm correspondingly. The ratios V_{out}/V_{in} are 3.2 ± 1.1 for simulations with explicit damping and 2.3 ± 0.4 for simulations without explicit damping. The amplitude ratio obtained from the observations (for the same averaging regions) equals 3.9 ± 1.0 . Thus, in both cases our simulations show that more than a half of the amplitude suppression comes from the absence of acoustic sources inside the sunspot, and the results are not much sensitive to the mechanism of wave damping. Our numerical experiments showed that amplitude ratio V_{out}/V_{in} is insensitive to the detailed shape of the profile of the acoustic source strength. However, it is important that the FWHM of the source strength is close to the FWHM of the averaged horizontal amplitude profile of the observed wave field. We found that the amplitude ratio increases for smaller depth h_{src} of the acoustic sources and equals 5.5 ± 1.7 for $h_{src} = 100$ km below the photosphere (low top absorbing boundary without explicit damping). This can be an evidence that the depth of the acoustic sources is between 100 km and 350 km, if the absence of acoustic sources is a dominating mechanism of the amplitude suppression in sunspots.

We have carried such simulations for several other sunspots, and obtained similar results. The comparison between simulations and observations for sunspots of different sizes is shown in Fig. 5a. The ratio V_{out}/V_{in} as a function of umbra diameter is plotted. The open circles represent observations, the stars represent simulations. Both the simulations and the observations show the same trend: the amplitude suppression increases with the size of sunspots. On average, the amplitude ratio is about a half of the observed one for the sources at depth 350 km, and higher for shallower sources. Frequency dependence of the amplitude ratio for AR8243 is shown in Fig. 5b. The frequency shift between the simulations and observations in Fig. 5b can be an evidence that the acoustic cut-off frequency inside sunspots is much lower than in the quiet Sun, but this requires further investigation.

This may be one of the additional factors which affect the oscillation amplitude in sunspots.

4. Discussion

We have carried numerical simulations of the effect of reduced excitation of solar oscillation in sunspot regions. The oscillations are excited by random sources, modeled as vertical momentum and pressure perturbations (in reality caused by turbulent convection). In sunspot regions, the wave sources are weaker because the magnetic field of sunspots inhibits convective motions. The results of simulations show that for a wide range of sunspot diameters more than a half of suppression of oscillation amplitude can be explained by the absence of acoustic sources in sunspots.

Our simulations also showed that the oscillation amplitude in regions of suppressed excitation only weakly depends on the wave damping mechanism in the upper convection zone and atmosphere as long as the line widths in the simulated power spectrum are close to the observed ones. We modeled wave damping by two methods: introducing a friction-type term into the z-component of the momentum equation and putting the wave absorbing boundary at various heights in the chromosphere. In both cases we get the similar ratios of oscillation amplitudes. If the acoustic cut-off frequency in sunspots is reduced this will increase the damping and may lead to even stronger reduction of the wave amplitude compared to the quiet Sun.

We thank Prof. P. Scherrer for fruitful discussions.

REFERENCES

- Cally, P. S. 1995, *ApJ*, 451, 372.
- Carpenter, M.H., Gottlieb, D., & Abarbanel, S. 1993, *J. Comput. Phys.* 108, 272.
- Christensen-Dalsgaard, J., et al. 1996, *Science*, 272, 1286.
- Christensen-Dalsgaard, J. & Frandsen, S. 1983, *SoPh*, 82, 165C.
- Gizon, L. & Birch, A. C. 2002, *ApJ*, 571, 966.
- Hindman, B. W. 1997, *ApJ*, 476, 392.
- Hu, F. Q. 1996, *J. Comput. Phys.*, 129, 201.

- Jones, H. P. 1989, *Sol. Phys.*, 120, 211.
- Kumar, P. & Basu, S. 2000, *ApJ*, 545, L65.
- Murawski, K. 2003, in R. Erdélyi, E. Forgács-Dajka, K. Petrovay (eds.), *Contributions on Turbulence, Waves and Instabilities in the Solar Plasma*, Publ. Astron. Dept. Eötvös Univ. 13, Budapest, p. 61.
- Nigam, R. & Kosovichev, A. G. 1999, *ApJ*, 514, L53.
- Parchevsky, K. V. & Kosovichev, A. G. 2006, arXiv:astro-ph/0612364 (*ApJ*, in press).
- Rogers, F. J., Swenson, F. J., & Iglesias, C. A. 1996, *ApJ*, 456, 902.
- Scherrer, P. H., et al. 1995, *Sol. Phys.*, 162, 129.
- Shu, C. W. 2002, in *Collected Lectures on the Preservation of Stability under Discretization*, eds. D. Estep & S. Tavener, SIAM, 51.
- Stein, R. F., & Nordlund, Å. 2001, *ApJ*, 546, 585.
- Tam, C. & Webb, J. 1993, *J. Comput. Phys.*, 107, 262.
- Thomas, J. H., Cram, L. E., & Nye, A. H. 1982, *Nature*, 297, 485.
- Title, A. M., et al. 1992, *ApJ*, 393, 782.
- Vernazza, J. E., Avrett, E. H., & Loeser, R. 1976, *ApJS*, 30, 1.
- Woods, D. T. & Cram, L. E. 1981, *Sol. Phys.*, 69, 233.

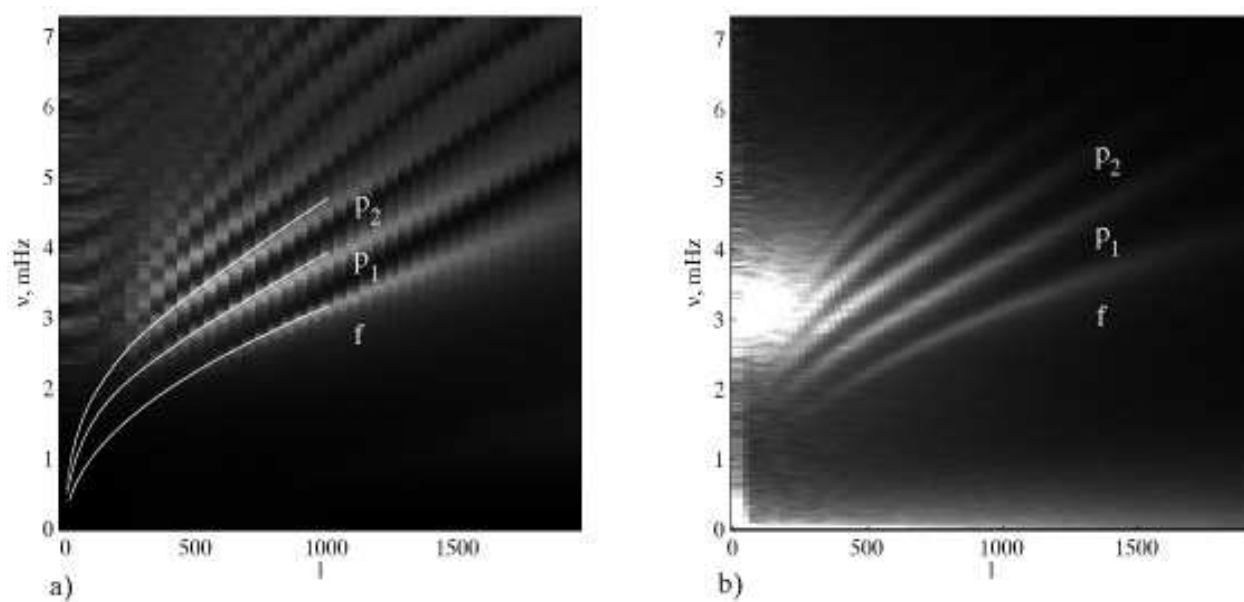


Fig. 1.— Power spectrum of the vertical component of velocity obtained from the simulations a) and high-resolution SOHO/MDI data b) (Scherrer et al. 1995). The acoustic spectral density depicted by a gray-scale is given in arbitrary units. The white curves show observed f , p_1 , and p_2 mode ridges; l is the angular degree.

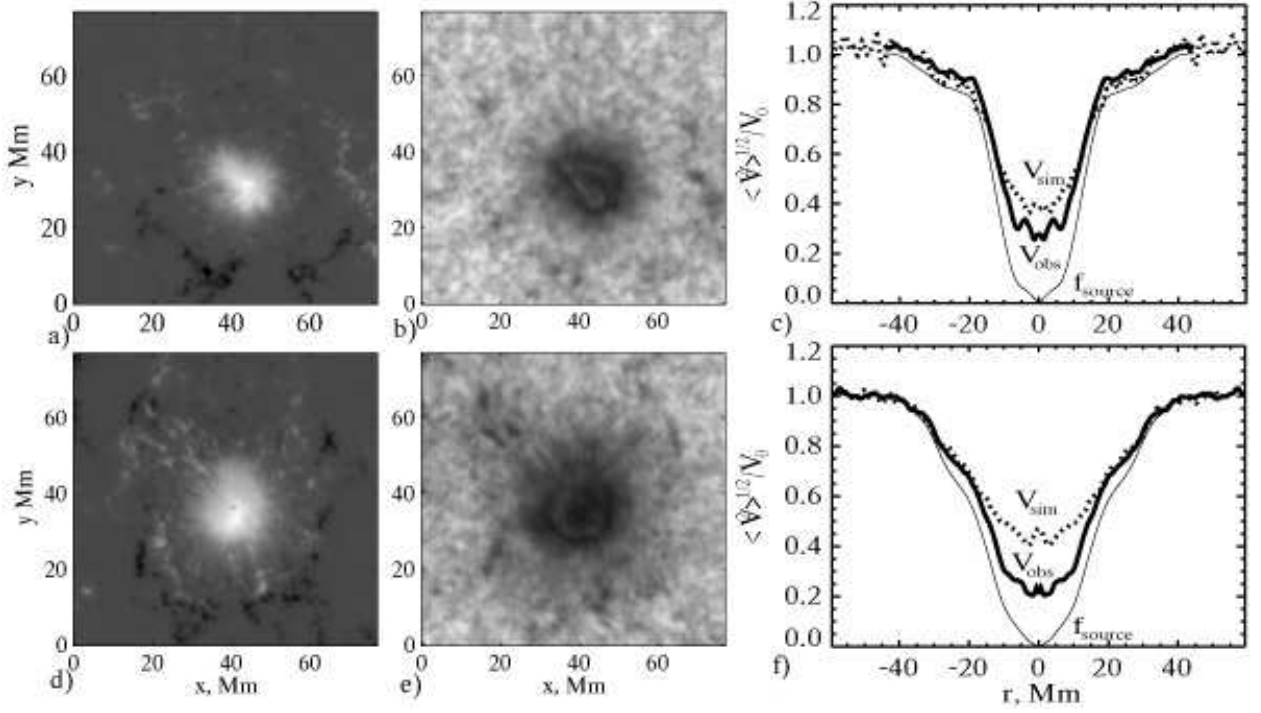


Fig. 2.— Panels a) and d) represent the line-of-sight magnetic field maps, panels b) and e) show the oscillation amplitude maps. The profiles of rms oscillation velocities at frequency 3.65 mHz for observations (thick solid curves), simulations (dashed curves), and the profiles of source strength (thin solid curves) for sunspots in two active regions AR10373 (top) and AR8243 (bottom) are shown in panels c) and f).

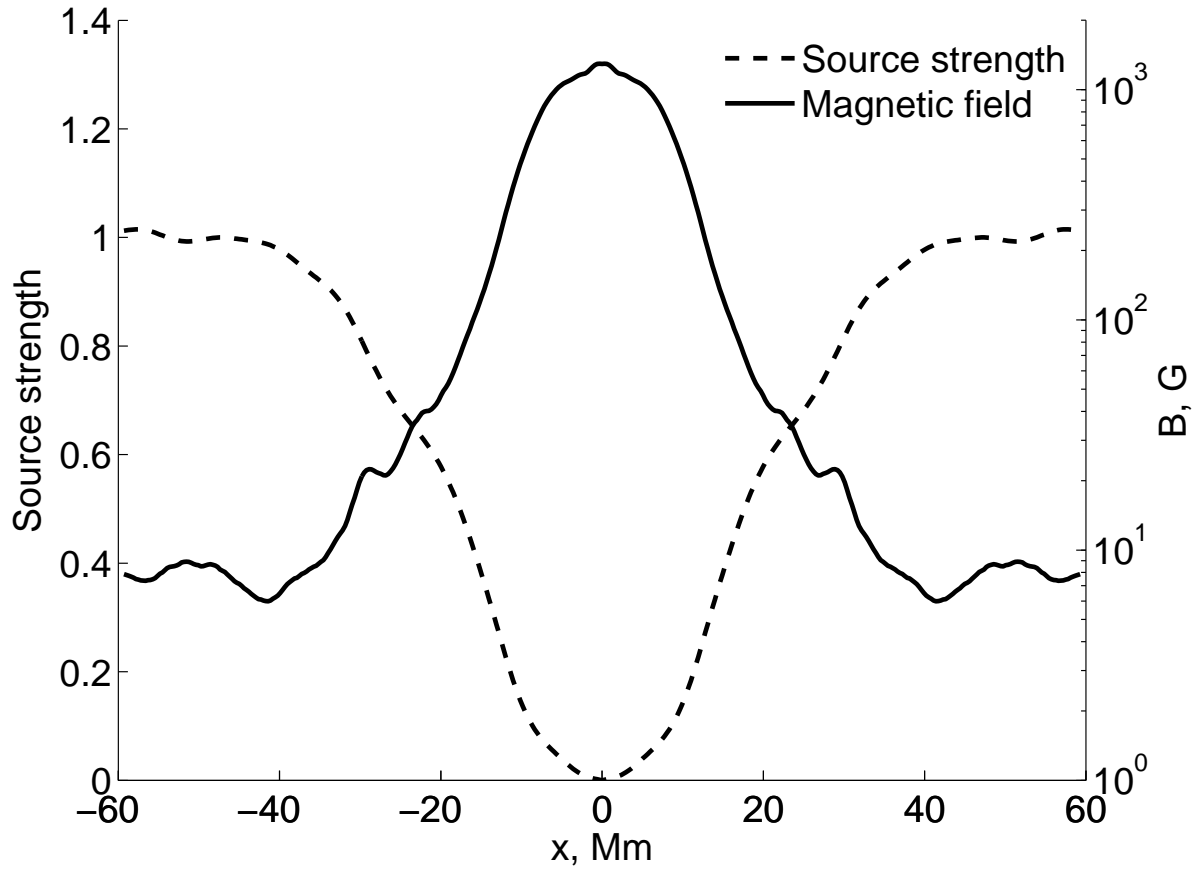


Fig. 3.— Horizontal profiles of the source strength (dashed curve) and angular averaged magnetic field strength (solid curve).

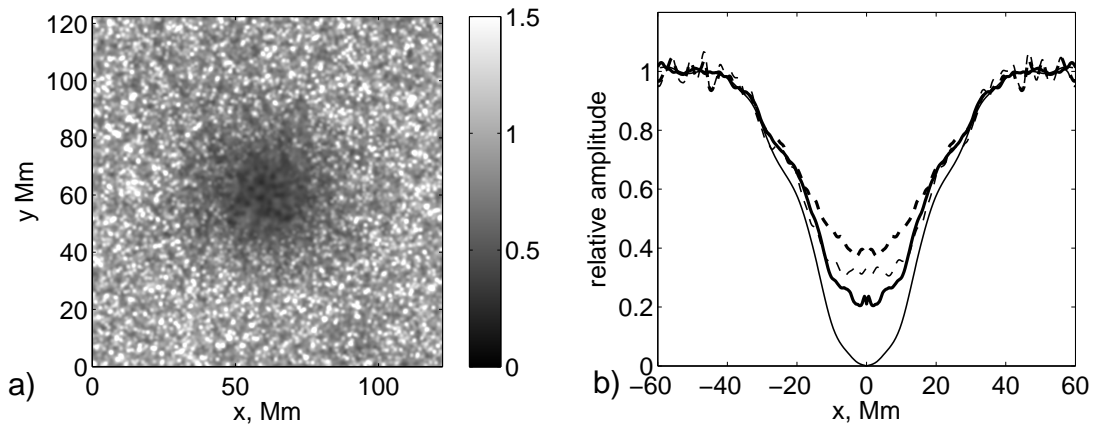


Fig. 4.— Vertical velocity oscillation amplitude map for the atmospheric damping a). Angular averaged amplitude profiles obtained from simulations are shown in panel b) by the thick dashed curve for atmospheric damping and the thin dashed curve for explicit damping. The thin solid curve represents the source strength profile calculated from observations of the sunspot in AR8243. The thick solid curve shows the observational amplitude profile for the same sunspot.

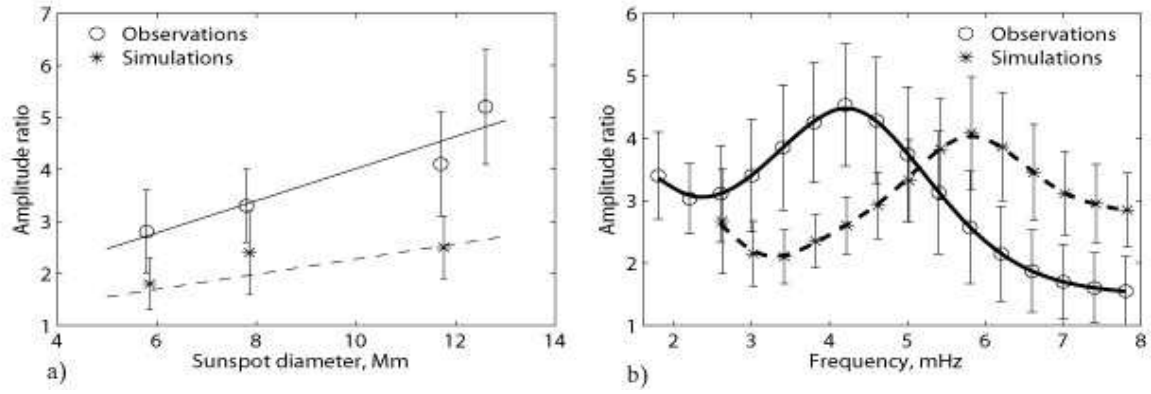


Fig. 5.— Ratio of the oscillation amplitudes of the vertical velocity V_{out}/V_{in} as a function of umbra diameter a) and frequency dependence of the amplitude ratio for the sunspot in AR8243 b).